Published in final edited form as:
Exp Biol Med (Maywood). 2010 May ; 235(5): 633–641. doi:10.1258/ebm.2009.009229.

The iron chelator, desferrioxamine, reduces inflammation and atherosclerotic lesion development in experimental mice

Wei-Jian Zhang[1,2,*], **Hao Wei**[1], and **Balz Frei**[1,2,*]

[1] Linus Pauling Institute, Oregon State University, Corvallis, OR 97331, USA

[2] Department of Biochemistry and Biophysics, Oregon State University, Corvallis, OR 97331, USA

Abstract

Objective—Vascular inflammation and monocyte recruitment are initiating events in atherosclerosis that have been suggested to be caused, in part, by iron-mediated oxidative stress and shifts in the intracellular redox environment of vascular cells. Therefore, the objective of this study was to investigate whether the intracellular iron chelator, desferrioxamine (DFO), reduces inflammation and atherosclerosis in experimental mice.

Methods and Results—Treatment of C57BL/6J mice with DFO (daily i.p. injection of 100 mg/kg body weight for two weeks) strongly inhibited lipopolysaccharide-induced increases of soluble cellular adhesion molecules and monocyte chemoattractant protein-1 (MCP-1) in serum and activation of the redox-sensitive transcription factors, nuclear factor κB and activator protein-1, in aorta. Furthermore, treatment of apolipoprotein E-deficient (apoE−/−) mice with DFO (100 mg/kg, i.p., daily for ten weeks) attenuated aortic atherosclerotic lesion development by 26% ($P<0.05$). DFO treatment of apoE−/− mice also lowered serum levels of MCP-1 and gene expression of pro-inflammatory and macrophage markers in aorta and heart, in parallel with increased protein expression of the transferrin receptor in the heart and liver. In contrast, DFO treatment had no effect on serum cholesterol and triglyceride levels.

Conclusions—These data show that DFO inhibits inflammation and atherosclerosis in experimental mice, providing the proof-of-concept for an important role of iron in atherogenesis. Whether eliminating excess iron is a useful adjunct for the prevention or treatment of atherosclerosis in humans remains to be seen.

Keywords

atherosclerosis; inflammation; iron chelation; redox-active transition metals

INTRODUCTION

Atherosclerosis is a chronic inflammatory disease initiated by the interaction of circulating monocytes with activated vascular endothelial cells that express adhesion molecules and other pro-inflammatory mediators, such as vascular cell adhesion molecule-1 (VCAM-1), intercellular adhesion molecule-1 (ICAM-1), and monocyte chemoattractant protein-1

[*]Correspondence and reprint requests should be addressed to: Wei-Jian Zhang and Balz Frei, Linus Pauling Institute, Oregon State University, 571, Weniger Hall, Corvallis, OR 97331, USA, Phone: 1-541-737-5075, FAX: 1-541-737-5077, weijian.zhang@oregonstate.edu and balz.frei@oregonstate.edu.

DISCLOSURE/CONFLICT OF INTEREST
There is NO conflict of interest to disclose.

(MCP-1) (1). Once in the intimal subendothelial space, the monocytes differentiate into macrophages and–upon scavenger receptor-mediated uptake and phagocytosis of modified LDL–are transformed into lipid-laden foam cells, the hallmark of the early atherosclerotic fatty streak.

The potential contribution of infection to the induction and progression of atherosclerosis is being increasingly recognized (2). Animal studies have shown that lipopolysaccharide (LPS) plays a significant role in the development of atherosclerotic lesions in mice (3–6). Furthermore, increased expression of the toll-like receptor 4 has been detected in human atherosclerotic lesions (7,8). These data indicate that chronic infection and inflammation are key factors in the development of atherosclerosis.

Iron is the most abundant transition metal in mammalian cells and is essential for the physiological function of many proteins (9). However, excess or non-protein bound (labile) iron can be detrimental because it promotes the generation of free radicals and reactive oxygen species (ROS). Iron-mediated ROS production may cause oxidative damage to biological macromolecules and alter intracellular redox environment, thereby affecting redox-sensitive cell signaling pathways and transcription factors (10,11).

There is accumulating, albeit controversial, evidence that iron plays an important role in the pathogenesis of atherosclerosis. The association between body iron status and CVD risk was first postulated in the early 1980s (12) and is supported by numerous epidemiological studies (13,14). Catalytically-active iron has been detected in both early and advanced atherosclerotic lesions (15). However, a systematic review of 12 prospective cohort studies concluded that there are no strong associations between iron status and CVD risk (16). A recent randomized trial of mild iron reduction therapy found no significant cardiovascular benefit in elderly patients with established peripheral vascular disease; however, in the youngest quartile at entry there were highly significant reductions in all cause mortality and in combined death plus non-fatal myocardial infarction and stroke in association with iron reduction therapy (17). Some animal studies found that the severity of atherosclerosis is either enhanced by iron overload (18) or reduced by iron deficiency (19) or iron chelation (20). However, other studies have shown that iron overload decreases atherosclerosis in conjunction with a hypo- or hypercholesterolemic effect (21,22). We and others have shown that iron status affects vascular endothelial inflammation (23,24), and desferrioxamine (DFO), a ferric iron chelator, inhibits TNFα-induced expression of adhesion molecules in human aortic endothelial cells (23). We also reported that DFO inhibits LPS-induced superoxide production by NADPH oxidase *in vivo* (25). The main objective of this study was to investigate whether DFO treatment reduces inflammation and inhibits atherosclerotic lesion development in two murine models.

MATERIALS AND METHODS

Animals and experimental procedures

Female C57BL/6J mice, 10–12 weeks old and weighing 20–22 g, and female apolipoprotein E-deficient (apoE−/−) mice on a C57BL/6J background, 4–5 weeks old and weighing 12–15 g, were purchased from Jackson Laboratory (Bar Harbor, ME). The investigation conformed to the *Guide for the Care and Use of Laboratory Animals* (NIH Publication No. 85–23, revised 1996) and was approved by Oregon State University's Institutional Animal Care and Use Committee.

For experiments investigating acute inflammation, four groups of C57BL/6J mice, fed *ad libitum* with Purina 5001 chow diet (Harlan Teklad, Madison, WI), were used: control animals receiving daily i.p. injections of the vehicle, Hanks' balanced salt solution (HBSS,

Sigma-Aldrich, St. Louis, MO), for 14 days; DFO-treated animals receiving daily i.p. injections of 100 mg/kg body weight (b.w.) of DFO (Novartis Pharmaceuticals, East Hanover, NJ) in HBSS for 14 days; LPS-treated animals receiving daily HBSS injections for 14 days, followed by a single i.p. injection of 50 μg LPS (serotype 055:B5 from *Escherichia coli,* Sigma-Aldrich); and DFO and LPS-treated animals receiving daily i.p. injections of 100 mg/kg b.w. of DFO in HBSS for 14 days, followed by a single i.p. injection of 50 μg LPS. Three hours after LPS injection or the last HBSS injection (control and DFO-treated mice) the animals were sacrificed, and blood and tissues were collected.

For experiments investigating atherosclerosis, apoE−/− mice were divided into two groups (n=18/group): control animals receiving daily i.p. injections of HBSS for ten weeks; and DFO-treated animals receiving daily i.p. injections of 100 mg/kg b.w. DFO in HBSS for ten weeks. Mice were fed *ad libitum* with a Western-type chow diet (No. 311372, Dyets Inc., Bethlehem, PA) containing 15% hydrogenated coconut oil and 0.125% cholesterol. For comparison, a group of five C57BL/6J mice, fed *ad libitum* with Purina 5001 chow diet containing 4% hydrogenated coconut oil, was used. At the end of the treatment period, all animals were sacrificed and perfused with 10 ml HBSS through the left ventricle of the heart, and heart and aorta were collected and processed as described below. Blood was collected and serum stored at −80°C until analysis.

Serum inflammatory mediators

Serum concentrations of sVCAM-1, MCP-1, and TNFα were measured by quantitative colorimetric sandwich ELISA (R&D Systems, Minneapolis, MN), and serum sICAM-1 using an ELISA kit from Endogen Inc. (Woburn, MA). The sensitivity of the assays is 30 pg/ml sVCAM-1, 5 ng/ml sICAM-1, 2 pg/ml MCP-1, and 5 pg/ml TNFα.

Serum total iron, ferritin, and lipids

Serum total iron and unsaturated iron binding capacity (UIBC) were measured spectrophotometrically using Ferrozine (Diagnostic Chemicals Ltd., Oxford, CT). Serum ferritin was determined by quantitative colorimetric sandwich ELISA (Immunology Consultants Laboratory, Newberg, OR). Serum total cholesterol and triglycerides were determined with colorimetric kits (Pointe Scientific, Inc., Canton MI).

Liver iron

Liver iron was measured using Inductively Coupled Plasma-Mass Spectrometry (ICP-MS). Liver samples were weighed and digested in 50% nitric acid at 70°C overnight. The digested samples were diluted 200-fold, and iron was measured in a PQ ExCell ICP-MS detector from Thermo Elemental (Waltham, MA). Indium was used as internal control. Iron standard was purchased from Ricca Chemical Company (Arlington, TX).

Western blots

Liver samples were homogenized in 1 ml lysis buffer (Cell Signaling Technology, Beverly, MA) followed by centrifugation at 14,000 g and 4°C for 15 min. The supernatant containing solubilized proteins was recovered, frozen in aliquots, and stored at −80°C until analysis. Protein samples were separated by 10% SDS-PAGE and transferred to nitrocellulose membranes. The membranes were incubated overnight with mouse anti-transferrin receptor antibody (Invitrogen, Carlsbad, CA) or rabbit anti-α-tubulin antibody (Cell Signaling, Danvers, MA), after blocking with 0.1% Tween 20 in Tris-buffered saline containing 5% skim milk powder. The membranes were incubated with HRP-conjugated goat anti-mouse antibody (Santa Cruz Biotechnology, Santa Cruz, CA) or goat anti-rabbit antibody (Cell

Signaling) for 1 h at room temperature. The proteins were detected by enhanced chemiluminescence (ECL^{TM}, GE Healthcare, Buckinghomshire, UK).

Real-time PCR

Total RNA was isolated from aorta and heart using TRIzol Reagent (Invitrogen). cDNA synthesis was performed using the high capacity cDNA archive kit from Applied Biosystems (Foster City, CA). mRNA levels of VCAM-1, ICAM-1, MCP-1, TNFα, IL-6, CD68, and glyceraldehyde-3-phosphate dehydrogenase (GAPDH) were quantitated by real-time PCR. All primers and probes were purchased as kits (Assays on Demand, Applied Biosystems). The assays are supplied as a 20x mixture of PCR primers and TaqMan minor groove binder 6-FAM dye labeled probes with a non-fluorescent quencher at the 3' end. TaqMan quantitative PCR (40 cycles at 95°C for 15 sec and 60°C for 1 min) was performed using TaqMan Universal PCR Master Mix (Applied Biosystems) in 96-well plates with the ABI Prism 7500 Sequence Detection System (Applied Biosystems). To obtain relative quantitation, two standard curves were constructed in each plate with one target gene and an internal control gene (GAPDH). Standard curves were generated by plotting the threshold cycle number values against the log of the amount of input cDNA and used to quantitate the expression of the target genes and GAPDH in the same sample. After normalization to internal GAPDH in each sample, results were expressed as percentage of GAPDH.

Nuclear transcription factors

Nuclear extracts were prepared from aortas using nuclear extract kits (Active Motif, Carlsbad, CA). For analysis of nuclear transcription factor activation, ELISA-based assays (Active Motif) were used to determine the DNA binding activity of NFκB (p65) and AP-1 (c-fos). The specificity of binding was confirmed by competition with either wild-type or mutant oligonucleotides.

Atherosclerotic lesions

For analysis of aortic atherosclerotic lesions, the aortic arch and thoracic aorta were carefully removed from the animal under a dissecting microscope. Adventitial tissue was removed and then the aorta was fixed overnight in 10% neutral-buffered formalin. Subsequently, the aorta was opened longitudinally *in situ* along the ventral midline and pinned out flat on a black wax surface with 0.2-mm diameter stainless steel pins (Fine Science Tools, Foster City, CA). The aortas were stained with Sudan IV to confirm the sudanophilic (fatty) lesions. The images of the aorta were captured with a Nikon digital camera (Coolpix 990) mounted on a Nikon stereo microscope. The total aortic surface and atherosclerotic lesion areas were analyzed *en face* by computerized quantitative morphometry (Image Pro Plus, Media Cybernetics, Bethesda, MD), and the aortic lesion area was expressed as percentage of the total aortic area.

Statistical analysis

The data were calculated as means ± SEM and analyzed by unpaired Student's *t* test or ANOVA with Fisher PLSD post-hoc test. Statistical significance was set at $P<0.05$.

RESULTS

DFO inhibits LPS-induced increases in serum sVCAM-1, sICAM-1, and MCP-1 in C57BL/6J mice

In agreement with our previous findings (26), exposing C57BL/6J mice to 50 μg LPS (i.p.) for 3 hours significantly increased serum levels of sVCAM-1, sICAM-1, MCP-1, and TNFα (Fig. 1). Prior treatment of the animals for 14 days with 100 mg/kg/day of DFO (i.p.)

significantly (P<0.01) inhibited these LPS-induced inflammatory responses (Fig. 1A–C): sVCAM-1 levels were 741 ± 50 ng/ml in mice treated with DFO and LPS, compared to 1125 ± 34 ng/ml in animals treated with LPS only; sICAM-1 levels were 31.2 ± 1.2 μg/ml and 40.1 ± 3.4 μg/ml, respectively; and MCP-1 levels, 9.2 ± 7.4 ng/ml and 41.0 ± 9.2 ng/ml, respectively (n=5/group). However, DFO did not inhibit the LPS-induced increase in serum TNFα (Fig. 1D).

DFO inhibits LPS-induced NFκB and AP-1 activation in aorta of C57BL/6J mice

The redox-sensitive transcription factors, NFκB and AP-1, play prominent roles in LPS-induced transcriptional regulation of most inflammatory mediators. As shown in Fig. 2, treating mice with LPS strongly increased the DNA-binding activity of NFκB (p65) and AP-1 (c-fos) in aorta. Prior treatment of the mice with DFO significantly suppressed the LPS-induced DNA binding activity of NFκB and AP-1 by 30% and 75%, respectively, compared to animals treated with LPS only (P<0.05, n=5/group) (Fig. 2).

DFO does not affect body weight gain of apoE−/− mice

To investigate the possible inhibitory effect of iron chelation by DFO on vascular inflammation and atherosclerotic lesion development, we used apoE−/− mice fed a high-fat/high-cholesterol diet. Body weights were checked biweekly during the ten-week treatment period. All animals continued to gain weight, and no statistically significant differences (by ANOVA) were observed between the control and DFO-treated animals (n=18/group): Body weights at baseline were 14.1±0.4 g for control mice and 13.8±0.5 g for DFO-treated mice, and 22.3±0.3 g and 21.5±0.4 g after ten weeks of treatment, respectively.

Effect of DFO on iron status of mice

Treatment of C57BL/6J mice with DFO for 14 days did not alter hemoglobin levels (control mice, 15.1±0.2 g/dl; DFO-treated mice, 15.0±0.3 g/dl) or hematocrit (control mice, 48.1±0.8%; DFO-treated mice, 46.8±0.8%, n=4–5/group). Treatment of apoE−/− mice with DFO also did not affect serum levels of total iron (control mice, 116.7±14.9 μg/dl; DFO-treated mice, 112.9±5.3 μg/dl; n=18/group) and UIBC (control mice, 287±14.1 μg/dl; DFO-treated mice, 254±11.3 μg/dl; n=18/group), but significantly (P<0.05) increased serum transferrin iron saturation (control mice, 37.8 ±1.7%; DFO-treated mice, 47.9±2.3%; n=18/group). Serum ferritin was unchanged (control mice, 438±88.0 ng/ml; DFO-treated mice, 514±36.1 ng/ml; n=18/group). In contrast, DFO significantly (P<0.01) reduced liver iron levels by 38% compared to non-DFO treated animals (control mice, 93±2.3 μg/g tissue; DFO-treated mice, 58±1.9 μg/g tissue; n=5/group). Interestingly, DFO treatment significantly (P<0.01) increased protein levels in the heart and liver of the transferrin receptor (TfR), a sensitive and reliable marker of intracellular iron status, by 2.1±0.4 and 4.0±0.4-fold, respectively, compared to control mice (n=3–4/group) (Fig. 3).

DFO does not change total cholesterol and triglycerides but lowers MCP-1 in serum of apoE−/− mice

While serum levels of total cholesterol and triglycerides were much higher (P<0.001) in apoE−/− mice (fed 15% hydrogenated coconut oil and 0.125% cholesterol) than C57BL/6J wild-type mice (fed a normal chow diet), they were not affected by DFO treatment of apoE −/− mice. Serum total cholesterol was 1031 ± 55 mg/dl in apoE−/− mice treated with DFO, compared to 960 ± 48 mg/dl in control apoE−/− mice; serum triglycerides were 105.8 ± 4.3 mg/dl and 105.6 ± 4.6 mg/dl, respectively. Serum levels of MCP-1, sVCAM-1, sICAM-1, and TNFα also were significantly higher (P<0.01) in apoE−/− mice than wild-type mice (Fig. 4). While DFO-treated apoE−/− mice exhibited significantly lower (P<0.01) serum MCP-1 levels than control apoE−/− mice (40 ± 3 pg/ml and 65 ± 5 pg/ml, respectively;

n=18/group) (Fig. 4C), serum levels of sVCAM-1, sICAM-1, and TNFα did not differ between the two groups (Fig. 4A, B and D).

DFO inhibits aortic atherosclerotic lesion development in apoE−/− mice

By the end of the ten-week treatment period, apoE−/− mice had developed widespread atherosclerotic lesions in the aortic arch and thoracic aorta. The extent of atherosclerosis was quantified using *en face* analysis of the whole aorta. As shown in Fig. 5, DFO treatment significantly ($P<0.05$) reduced atherosclerosis by 26% compared to non-DFO treated control animals. The lesion area in apoE−/− mice was 7.10±0.48% of total aorta in the control group and 5.27±0.37% in the DFO-treated group (n=8/group).

DFO inhibits inflammatory and macrophage-specific gene expression in heart and aorta of apoE−/− mice

Gene expression of VCAM-1, ICAM-1, MCP-1, TNFα, and IL-6 was significantly higher ($P<0.05$) in apoE −/− mice than wild-type mice (n=5/group). DFO treatment of apoE−/− mice significantly ($P<0.05$) reduced mRNA levels in the heart by 20% (VCAM-1), 29% (ICAM-1), 64% (MCP-1), 62% (TNFα), and 54% (IL-6) compared to non-DFO treated apoE−/−mice (n=5/group) (Fig. 6B). In aorta, expression of the same inflammatory genes also was lower in the DFO-treated *vs*. non- treated mice, but the differences did not quite reach statistical significance (Fig. 6A).

As macrophage accumulation in the arterial wall critically contributes to atherosclerotic lesion development, we investigated gene expression of the macrophage marker, CD68. Treatment of animals with DFO significantly ($P<0.05$) lowered CD68 gene expression in both aorta (Fig. 6A) and heart (Fig. 6B) by 40% and 24%, respectively, compared to non-DFO treated apoE−/− mice (n=5/group).

DISCUSSION

Vascular inflammation plays a central role in the complex chain of events leading to atherosclerotic lesion development (1,27). There is accumulating, although controversial, evidence that redox-active transition metal ions such as iron or copper are causative agents in the pathogenesis of atherosclerosis and its clinical sequelae (15,28). Thus, intracellular metal chelation may have anti-atherogenic effects and improve cardiovascular outcome (29,30). In this study, we found that the iron chelator, desferrioxamine, reduces inflammation in LPS-exposed C57BL mice and inhibits inflammation and atherosclerotic lesion development in the aorta of apoE−/− mice.

Reactive oxygen species have been implicated as key mediators of cell signaling pathways that activate redox-sensitive transcription factors, which in turn upregulate inflammatory gene expression (31). It has been shown that ROS production and LDL oxidation by cultured vascular cells are mediated by transition metal ions (32,33), and the oxidative capacity of these cells is greatly enhanced by micromolar concentrations of iron (24,34). In addition, LPS and iron may enhance cellular superoxide production by increasing NADPH oxidase activity (25). Catalytic or labile iron also has been shown to induce inflammatory responses in vascular endothelial cells, as manifested, *e.g*., by increased expression of adhesion molecules and IL-6 and increased adherence of monocytes to these cells (24).

Therefore, removal of intracellular labile iron may decrease ROS production and oxidative stress, thereby diminishing cell and tissue injury and inflammatory responses. In agreement with this notion, the iron chelator, DFO, has been shown to effectively inhibit iron-mediated ROS production *in vitro* and *in vivo* (35–37) and protect cells from H_2O_2-induced DNA damage (38). Furthermore, DFO can protect against ROS-induced myocardial and coronary

endothelial ischemia-reperfusion injury (39,40) and improve endothelium-dependent vasodilation in CVD patients (41). Consistent with these observations, our data show that DFO inhibits LPS-induced acute inflammatory responses *in vivo*, as evidenced by reduced serum levels of adhesion molecules and MCP-1 and decreased aortic NFκB and AP-1 activation.

As explained, inflammation and oxidative stress in the arterial wall are prominent features of atherosclerosis. Ross (1) observed that feeding an atherogenic diet to experimental animals induced adhesion of monocytes and other inflammatory cells to the arterial wall in a matter of days. The antioxidant and anti-inflammatory effects of DFO most likely account for its observed anti-atherogenic effect in apoE−/− mice in the present study, which is in agreement with an earlier report that DFO decreases atherosclerotic lesion development in cholesterol-fed rabbits (20). In our study, DFO not only inhibited aortic atherosclerosis, but also significantly decreased macrophage accumulation, as assessed by CD68 expression. Aortic gene expression of MCP-1, a chemokine that plays a critical role in vascular monocyte recruitment and atherogenesis (1), was markedly–albeit non-significantly–reduced by DFO. In addition, DFO treatment significantly decreased gene expression of VCAM-1, ICAM-1, MCP-1, TNFα, and IL-6 in the heart, which is compatible with the notion of decreased inflammation and atherosclerotic lesion development in coronary arteries. We also found that DFO significantly increased tissue expression of TfR in heart and liver, a sensitive and reliable marker of intracellular labile iron status. While these data cannot establish cause-and-effect, they suggest that (intracellular) iron plays a critical role in inflammation and atherosclerosis, and that iron chelation by DFO inhibits atherosclerotic lesion development, in part, by suppressing vascular inflammation and monocyte-macrophage recruitment.

The finding that DFO exerted anti-inflammatory effects in apoE−/− mice is further buttressed by our observations that DFO suppressed LPS-induced acute inflammatory responses in C57BL mice and inhibited TNFα-induced expression of adhesion molecules and MCP-1 in human aortic endothelial cells (23). These studies also revealed a common underlying mechanism for the anti-inflammatory effect of DFO, *viz*., inhibition of NFκB activation, a redox-sensitive transcription factor that regulates expression of many inflammatory genes (11). In most cell types, NFκB can be activated by a diverse range of stimuli, suggesting that several signaling pathways are involved. Lipid peroxidation has been reported to play a role in TNFα-induced NFκB activation (42). Redox-active transition metal ions play a key role in the initiation and propagation of lipid peroxidation, leading to the generation of peroxyl and alkoxyl radicals, as well as lipid hydroperoxides and numerous reactive breakdown products (33). DFO, which strongly inhibits iron-dependent lipid peroxidation, also strongly inhibited TNFα-induced NFκB activation in endothelial cells (42). Consistent with these data, in the present *in vivo* study we found that DFO treatment strongly inhibited LPS-induced NFκB activation in aorta.

The macrophage is a key cell type in the formation and fate of an atherosclerotic plaque. The accumulation of iron by plaque macrophages, mainly via erythrophagocytosis, promotes lipid uptake by stimulating expression of the macrophage scavenger receptor–1 (43). Oxidative reactions associated with the acquisition of iron and lipid may facilitate macrophage apoptosis, with the release of their cellular content into the atherosclerotic lesion. The release of iron and lipids contributes to the cellular mass of the lesion and causes further monocyte recruitment to the arterial wall, thereby amplifying the atherosclerotic process. Interruption of iron acquisition and storage in plaque macrophages by iron restriction or iron chelation inhibits lesion initiation and progression (19,20). In agreement with these observations, our results provide new evidence that DFO treatment inhibits macrophage accumulation in the arterial wall.

It should be noted that large doses of DFO appear to be safe in experimental animals, *e.g.*, 540 mg/kg/d for 7 days in rats (44) and 170 mg/kg/d in mice (45). Our preliminary data also showed that DFO at a daily dose of 500 mg/kg for seven days exerted no toxic effects. In our study, treating apoE−/− mice for 10 weeks with 100 mg/kg/d DFO did not cause significant growth retardation or body weight loss. Consistent with previous reports (20,46), we found that DFO did not affect serum iron, ferritin, and hemoglobin levels, as well as hematocrit. Hence, mice treated with DFO likely had sufficient iron stores to maintain normal erythropoiesis. However, we did find that DFO significantly decreased liver iron levels and increased cardiac and hepatic TfR expression, indicating that DFO effectively depleted tissue iron stores.

In conclusion, our study indicates that the iron chelator, DFO, inhibits inflammation and atherosclerotic lesion development in experimental mice, and provides the proof-of-concept that iron plays an important role in the pathogenesis of atherosclerosis. The relationship between iron stores and CVD in humans and the potential benefits of chelation of excess iron or limiting iron intake as a complementary strategy to prevent or treat atherosclerosis in humans requires further investigation.

Acknowledgments

WJZ and BF designed research; WJZ and HW conducted the experiments; WJZ and BF analyzed data and wrote the manuscript.

Grant numbers and sources of support: This work was supported by a pilot project grant from the Linus Pauling Institute [to WJZ] and grant number P01 AT002034 [to BF and WJZ] from the National Center for Complementary and Alternative Medicine (NCCAM).

References

1. Ross R. Atherosclerosis – an inflammatory disease. N Engl J Med 1999;340:115–126. [PubMed: 9887164]
2. Epstein SE, Zhu J, Najafi AH, Burnett MS. Insights into the role of infection in atherogenesis and in plaque rupture. Circulation 2009;119:3133–3141. [PubMed: 19546396]
3. Ostos MA, Recalde D, Zakin MM, Scott-Algara D. Implication of natural killer T cells in atherosclerosis development during a LPS-induced chronic inflammation. FEBS Lett 2002;519:23–29. [PubMed: 12023012]
4. Cuaz-Pérolin C, Billiet L, Baugé E, Copin C, Scott-Algara D, Genze F, Büchele B, Syrovets T, Simmet T, Rouis M. Antiinflammatory and antiatherogenic effects of the NF-kappaB inhibitor acetyl-11-keto-beta-boswellic acid in LPS-challenged ApoE−/− mice. Arterioscler Thromb Vasc Biol 2008;28:272–277. [PubMed: 18032778]
5. Westerterp M, Berbée JF, Pires NM, van Mierlo GJ, Kleemann R, Romijn JA, Havekes LM, Rensen PC. Apolipoprotein C-I is crucially involved in lipopolysaccharide-induced atherosclerosis development in apolipoprotein E-knockout mice. Circulation 2007;116:2173–181. [PubMed: 17967778]
6. Gitlin JM, Loftin CD. Cyclooxygenase-2 inhibition increases lipopolysaccharide-induced atherosclerosis in mice. Cardiovasc Res 2009;81:400–407. [PubMed: 18948273]
7. Edfeldt K, Swedenborg J, Hansson GK, Yan ZQ. Expression of toll-like receptors in human atherosclerotic lesions: a possible pathway for plaque activation. Circulation 2002;105:1158–1161. [PubMed: 11889007]
8. Vink A, Schoneveld AH, van der Meer JJ, van Middelaar BJ, Sluijter JP, Smeets MB, Quax PH, Lim SK, Borst C, Pasterkamp G, de Kleijn DP. In vivo evidence for a role of toll-like receptor 4 in the development of intimal lesions. Circulation 2002;106:1985–1990. [PubMed: 12370224]
9. Papanikolaou G, Pantopoulos K. Iron metabolism and toxicity. Toxicol App Pharmacol 2005;202:199–211.

10. Welch KD, Davis TZ, Van Eden ME, Aust SD. Deleterious iron-mediated oxidation of biomolecules. Free Radic Biol Med 2002;32:577–583. [PubMed: 11909692]
11. Flohé L, Brigelius-Flohé R, Saliou C, Traber MG, Packer L. Redox regulation of NF-kappa B activation. Free Radic Biol Med 1997;22:1115–1126. [PubMed: 9034250]
12. Sullivan JL. Iron and sex difference in heart disease risk. Lancet 1981;1:1293–1294. [PubMed: 6112609]
13. Salonen JT, Nyyssonen K, Korpela H, Tuomilehto J, Seppanen R, Salonen R. High stored iron levels are associated with excess risk of myocardial infarction in eastern Finnish men. Circulation 1992;86:803–811. [PubMed: 1516192]
14. Kiechl S, Willeit J, Egger G, Poewe W, Oberhollenzer F. Body iron stores and the risk of carotid atherosclerosis: prospective results from the Bruneck study. Circulation 1997;96:3300–3307. [PubMed: 9396420]
15. Stadler N, Lindner RA, Davies MJ. Direct detection and quantification of transition metal ions in human atherosclerotic plaques: evidence for the presence of elevated levels of iron and copper. Arterioscler Thromb Vasc Biol 2004;24:949–954. [PubMed: 15001454]
16. Danesh J, Appleby P. Coronary heart disease and iron status: meta-analyses of prospective studies. Circulation 1999;99:852–854. [PubMed: 10027804]
17. Zacharski LR, Chow BK, Howes PS, Shamayeva G, Baron JA, Dalman RL, Malenka DJ, Ozaki CK, Lavori PW. Reduction of iron stores and cardiovascular outcomes in patients with peripheral arterial disease: a randomized controlled trial. JAMA 2007;297:603–610. [PubMed: 17299195]
18. Araujo JA, Romano EL, Brito BE, Parthe V, Romano M, Bracho M, Montano RF, Cardier J. Iron overload augments the development of atherosclerotic lesions in rabbits. Arterioscler Thromb Vasc Biol 1995;15:1172–1180. [PubMed: 7542998]
19. Lee TS, Shiao MS, Pan CC, Chau LY. Iron-deficient diet reduces atherosclerotic lesions in apoE-deficient mice. Circulation 1999;99:1222–1229. [PubMed: 10069791]
20. Minqin R, Rajendran R, Pan N, Tan BK, Ong WY, Watt F, Halliwell B. The iron chelator desferrioxamine inhibits atherosclerotic lesion development and decreases lesion iron concentrations in the cholesterol-fed rabbit. Free Radic Biol Med 2005;38:1206–1211. [PubMed: 15808418]
21. Dabbagh AJ, Shwaery GT, Keaney JF Jr, Frei B. Effect of iron overload and iron deficiency on atherosclerosis in the hypercholesterolemic rabbit. Arterioscler Thromb Vasc Biol 1997;17:2638–2645. [PubMed: 9409237]
22. Kirk EA, Heinecke JW, LeBoeuf RC. Iron overload diminishes atherosclerosis in apoE-deficient mice. J Clin Invest 2001;107:1545–1553. [PubMed: 11413162]
23. Zhang WJ, Frei B. Intracellular metal ion chelators inhibit TNFalpha-induced SP-1 activation and adhesion molecule expression in human aortic endothelial cells. Free Radic Biol Med 2003;34:674–682. [PubMed: 12633744]
24. Kartikasari AE, Georgiou NA, Visseren FL, van Kats-Renaud H, van Asbeck BS, Marx JJ. Intracellular labile iron modulates adhesion of human monocytes to human endothelial cells. Arterioscler Thromb Vasc Biol 2004;24:2257–2262. [PubMed: 15486315]
25. Li L, Frei B. Iron chelation inhibits NF-kappaB-mediated adhesion molecule expression by inhibiting p22 (phox) protein expression and NADPH oxidase activity. Arterioscler Thromb Vasc Biol 2006;26:2638–2643. [PubMed: 16973969]
26. Zhang WJ, Wei H, Frei B. Genetic impairment of NADPH oxidase does not diminish but rather enhances LPS-induced acute inflammatory responses *in vivo*. Free Radic Biol Med 2009;46:791–798. [PubMed: 19124074]
27. Stocker R, Keaney JF Jr. Role of oxidative modifications in atherosclerosis. Physiol Rev 2004;84:1381–478. [PubMed: 15383655]
28. Sullivan JL. Iron in arterial plaque: A modifiable risk factor for atherosclerosis. Biochim Biophys Acta 2009;1790:718–723. [PubMed: 18619522]
29. Marx JJ, Kartikasari AE, Georgiou NA. Can iron chelators influence the progression of atherosclerosis? Hemoglobin 2008;32:123–134. [PubMed: 18274990]
30. Tanner MA, Galanello R, Dessi C, Smith GC, Westwood MA, Agus A, Roughton M, Assomull R, Nair SV, Walker JM, Pennell DJ. A randomized, placebo-controlled, double-blind trial of the

effect of combined therapy with deferoxamine and deferiprone on myocardial iron in thalassemia major using cardiovascular magnetic resonance. Circulation 2007;115:1876–1884. [PubMed: 17372174]

31. Cuzzocrea S, Riley DP, Caputi AP, Salvemini D. Antioxidant therapy: a new pharmacological approach in shock, inflammation, and ischemia/reperfusion injury. Pharmacol Rev 2001;53:135–159. [PubMed: 11171943]
32. Martin A, Frei B. Both intracellular and extracellular vitamin C inhibit atherogenic modification of LDL by human vascular endothelial cells. Arterioscler Thromb Vasc Biol 1997;17:1583–1590. [PubMed: 9301639]
33. Halliwell B, Gutteridge JMC. Role of free radicals and catalytic metal ions in human disease: an overview. Methods Enzymol 1990;186:1–85. [PubMed: 2172697]
34. Morel DW, DiCorleto PE, Chisolm GM. Endothelial and smooth muscle cells alter low density lipoprotein in vitro by free radical oxidation. Arteriosclerosis 1984;4:357–364. [PubMed: 6466193]
35. Halliwell B. Protection against tissue damage in vivo by desferrioxamine: what is its mechanism of action? Free Radic Biol Med 1989;7:645–651. [PubMed: 2695408]
36. Halliwell B. Use of desferrioxamine as a 'probe' for iron-dependent formation of hydroxyl radicals. Evidence for a direct reaction between desferal and the superoxide radical. Biochem Pharmacol 1985;34:229–233. [PubMed: 2981536]
37. Marx JJ, van Asbeck BS. Use of iron chelators in preventing hydroxyl radical damage: adult respiratory distress syndrome as an experimental model for the pathophysiology and treatment of oxygen-radical-mediated tissue damage. Acta Haematol 1996;95:49–62. [PubMed: 8604586]
38. Doulias PT, Christoforidis S, Brunk UT, Galaris D. Endosomal and lysosomal effects of desferrioxamine: protection of HeLa cells from hydrogen peroxide-induced DNA damage and induction of cell-cycle arrest. Free Radic Biol Med 2003;35:719–728. [PubMed: 14583336]
39. Bolli R, Jeroudi MO, Patel PS, Aruoma OI, Halliwell B, Lai EK, McCay PB. Marked reduction of free radical generation and contractile dysfunction by antioxidant therapy begun at the time of reperfusion: evidence that myocardial ‘stunning' is a manifestation of reperfusion injury. Circ Res 1989;65:607–622. [PubMed: 2548761]
40. Sellke FW, Shafique T, Ely DL, Weintraub RM. Coronary endothelial injury after cardiopulmonary bypass and ischemic cardioplegia is mediated by oxygen-derived free radicals. Circulation 1993;88(suppl II):II395–400. [PubMed: 8222185]
41. Duffy SJ, Biegelsen ES, Holbrook M, Russell JD, Gokce N, Keaney JF Jr, Vita JA. Iron chelation improves endothelial function in patients with coronary artery disease. Circulation 2001;103:2799–2804. [PubMed: 11401935]
42. Bowie AG, Moynagh PN, O'Neill LA. Lipid peroxidation is involved in the activation of NF-kappaB by tumor necrosis factor but not interleukin-1 in the human endothelial cell line ECV304. Lack of involvement of H_2O_2 in NF-kappaB activation by either cytokine in both primary and transformed endothelial cells. J Biol Chem 1997;272:25941–25950. [PubMed: 9325328]
43. Kraml PJ, Klein RL, Huang Y, Nareika A, Lopes-Virella MF. Iron loading increases cholesterol accumulation and macrophage scavenger receptor I expression in THP-1 mononuclear phagocytes. Metabolism 2005;54:453–459. [PubMed: 15798950]
44. Bowern N, Ramshaw IA, Clark IA, Doherty PC. Inhibition of autoimmune neuropathological process by treatment with an iron-chelating agent. J Exp Med 1984;160:1532–1543. [PubMed: 6333485]
45. Bradley B, Prowse SJ, Bauling P, Lafferty KJ. Desferrioxamine treatment prevents chronic islet allograft damage. Diabetes 1986;35:550–555. [PubMed: 3082702]
46. Lalonde RG, Holbein BE. Role of iron in Trypanosoma cruzi infection of mice. J Clin Invest 1984;73:470–476. [PubMed: 6421877]

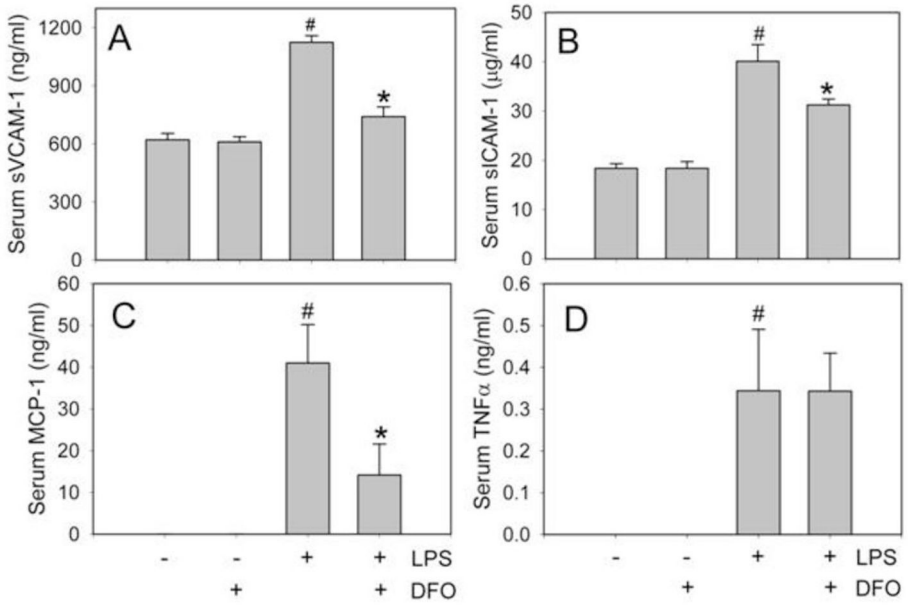

Fig. 1. DFO inhibits LPS-induced increases in serum sVCAM-1, sICAM-1, and MCP-1 in C57BL/6J mice

Mice were injected i.p. with vehicle HBSS (daily x 14 days), DFO (100 mg/kg b.w. daily x 14 days), 50 μg LPS, or LPS+DFO as described in Methods. Three hours after HBSS or LPS injection, the animals were sacrificed and blood was collected. Serum sVCAM-1 (A), sICAM-1 (B), MCP-1 (C), and TNFα (D) were measured by ELISA. Data shown are mean values ± SEM of five animals per group. $^{\#}P<0.01$ compared to control HBSS-treated animals and $^{*}P<0.01$ compared to LPS-treated animals.

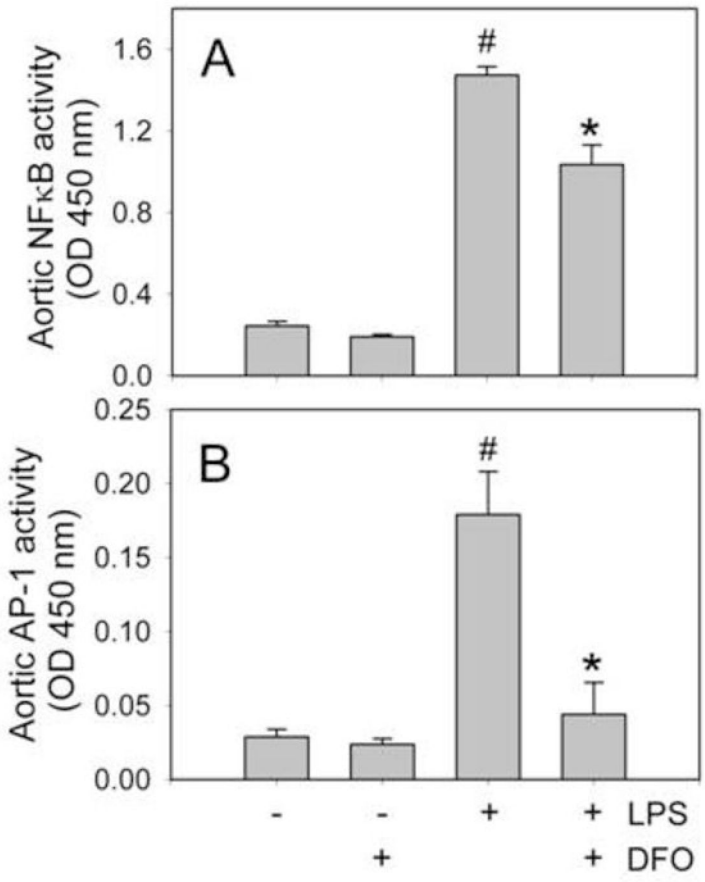

Fig. 2. DFO inhibits LPS-induced NFκB and AP-1 activation in aorta of C57BL/6J mice

Mice were injected i.p. with vehicle HBSS (daily x 14 days), DFO (100 mg/kg b.w. daily x 14 days), 50 μg LPS, or LPS+DFO as described in Methods. Three hours after HBSS or LPS injection, the animals were sacrificed and nuclear extracts were isolated from aorta. NFκB (p65)/DNA (A) and AP-1 (c-fos)/DNA (B) binding activities were quantified by ELISA. Data shown are mean values ± SEM of five animals per group. $^{\#}P<0.01$ compared to control HBSS-treated animals and $^{*}P<0.05$ compared to LPS-treated animals.

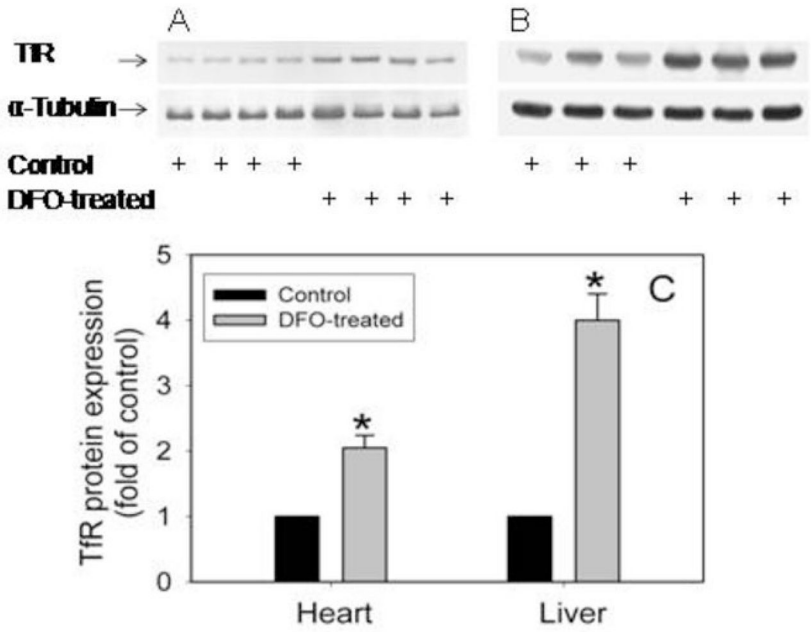

Fig. 3. DFO increases TfR expression in heart and liver of apoE−/− mice

ApoE−/− mice were daily injected i.p. with vehicle HBSS or DFO (100 mg/kg b.w.) for ten weeks as described in Methods. Heart (A) and liver (B) TfR protein was analyzed by Western blot as described in Methods. The intensity of the TfR bands was quantitated by densitometry and, after normalization to the α-tubulin protein, expressed as fold of control animals (C). Data shown are mean values ± SEM of 3–4 animals per group. *P<0.01 compared to control animals.

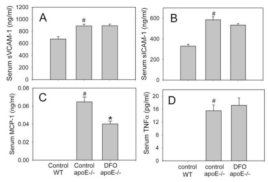

Fig. 4. DFO lowers serum MCP-1, but not sVCAM-1, sICAM-1 and TNFα, in apoE−/− mice

ApoE−/− mice were daily injected i.p. with vehicle HBSS or DFO (100 mg/kg b.w.) for ten weeks as described in Methods. Wild-type (WT) C57BL/6J mice were fed a normal chow diet. Serum levels of sVCAM-1 (A), sICAM-1(B), MCP-1 (C) and TNFα (D) were measured as described in Methods. Data shown are mean values ± SEM of 5 WT and 18 apoE−/− mice in each group. $^{\#}P<0.01$ compared to control WT animals and $^{*}P<0.01$ compared to control apoE−/− animals.

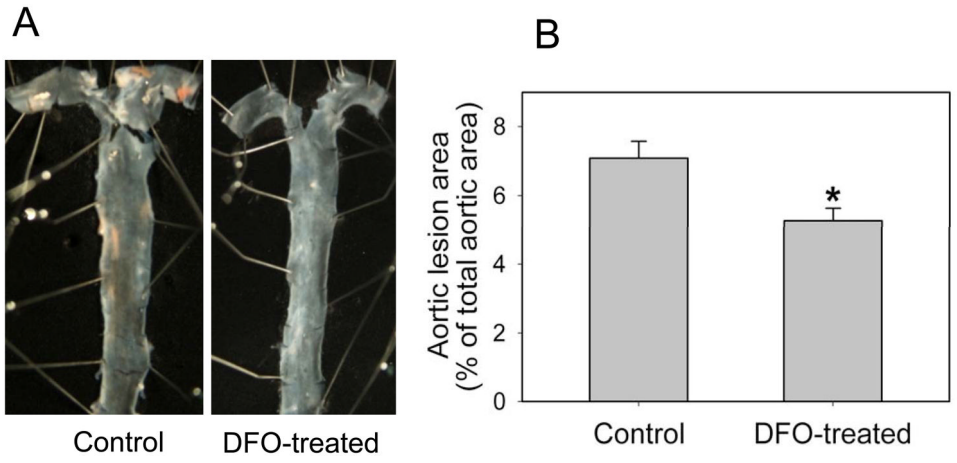

Fig. 5. DFO inhibits aortic atherosclerotic lesion development in apoE−/− mice

ApoE−/− mice were daily injected i.p. with vehicle HBSS or DFO (100 mg/kg b.w.) for ten weeks as described in Methods. (A) Pinned-out aortas from one representative animal of each group showing surface lesions (red areas). (B) Aortic surface lesion areas in control and DFO-treated mice were measured as described in Methods. Data shown are mean values ± SEM of 8 apoE−/− mice in each group. **P*<0.05 compared to control animals.

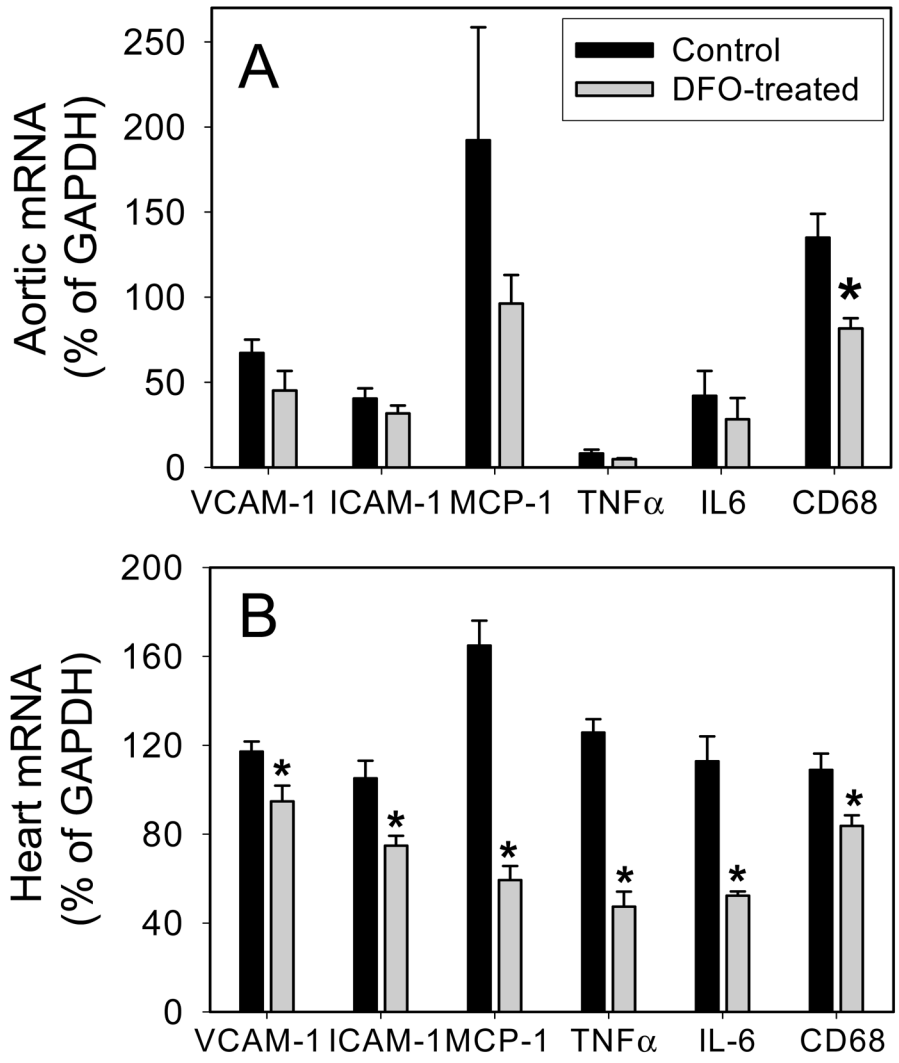

Fig. 6. DFO inhibits inflammatory and macrophage-specific gene expression in heart and aorta of apoE−/− mice

ApoE−/− mice were daily injected i.p. with vehicle HBSS (black bars) or DFO (100 mg/kg b.w.) (grey bars) for ten weeks as described in Methods. Total RNA was isolated from aorta (A) and heart (B), and VCAM-1, ICAM-1, MCP-1, TNFα, IL-6, CD68, and GAPDH mRNA levels were quantified using real-time quantitative PCR. After normalization to the internal control gene, GAPDH, the results for each target gene were calculated as percentage of GAPDH. Data shown are mean values ± SEM of five apoE−/− mice in each group. **P*<0.05 compared to control animals.